Beni-Suef University Journal of Basic and Applied Sciences

RESEARCH

Open Access

Synthesis and characterization of poly (styrene-co-acrylamide)-graft-polyanilines as new sorbents for mercuric present in aqueous hydrocarbon liquids

Hossam M. M. Fares[1], Eid. M. S. Azzam[2,3] and H. M. Abd El-Salam[1*]

Abstract

Background: The unprocessing hydrocarbon oil often contains high concentrations of mercury, which damages the metallic processing components and have health risk on workers and environment. Mercuric removal unit associated with natural gas processing plant is failed to complete mercury removal and then mercury distributed in most places of removal unit. Most of unremoved mercury are found in polar solutions.

Results: Styrene-co-acrylamide-graft-polyanilines were synthesized and characterized. The copolymer formed by free radical emulsion copolymerization of styrene-acrylamide (14:1) using ammonium persulphate (APS) at 60 °C. In addition, the grafting process was also achieved by oxidation chemical polymerization of the above copolymer with both aniline and 2-chloroaniline using APS. The synthetic polymeric samples were characterized using infrared (IR), x-ray diffraction (XRD), scan electron microscope (SEM), transition electron microscope (TEM), thermogravimetric analysis (TGA) and Brunauer–Emmett–Teller (BET) to confirm the polymerization process and investigate the polymeric samples as new sorbents for Hg (II). Both adsorption kinetics and isotherm models were checked.

Conclusions: In most cases Hg (II) was adsorbed as multi-layer on the obtained mesopores materials. The grafting process enhances the copolymer activity towards Hg (II) removal. The complete removal of mercury from water solution portion of mercuric removal unit was achieved by introduction of synthetic polymeric mesopores material based on styrene-co-acrylamide-graft-polyanilines. The removal efficiency closed to 100% in case of grafting with poly (2-chloroaniline).

Keywords: Mercury (II) removal, Free radical emulsion copolymerization, Styrene-co-acrylamide-graft-polyanilines, Aqueous hydrocarbon oil, Sorption

1 Background

Low concentrations of heavy metals can be profoundly poisonous and can amass in living beings, causing different diseases. Heavy metals are non-degradable like natural toxins. Once within the nourishment chain, they were concentrated in living organisms leading to high toxicity [1]. Mercury is considered one of the foremost poisonous heavy metals, because mercury capable of adsorbed via the skin, inward breath or by oral ways and produce antagonistic effects on human health [2]. Reactive mercury (II) is profoundly the most harmful shape of mercury which combine with the amino acid cysteine in proteins. Mercury (II) ions are considered as the most hazardous among different shapes of mercury due to their neurological harmfulness, persistence, volatility, and bio-accumulation through nourishment chain

*Correspondence: hanafya@yahoo.com; hanafy011246@science.bsu.edu.eg
[1] Department of Chemistry, Faculty of Science, Polymer Research Laboratory, Beni-Suef University, Beni-Suef City 62514, Egypt
Full list of author information is available at the end of the article

which has a real danger to both human health or human utilization and living being security [3].

Mercuric compounds listed in most classes of priority pollutants, so guidelines and regulations destined to limiting mercuric levels in the environment [4].

Mercury maximum level is confined to 1 μg/L and 1 $\mu g/m^3$ in both water and air according to World Health Organization (WHO) guidelines. Moreover, a permissible concentration of 0.2 $\mu g/m^3$ has been assessed according to the WHO for long-term inward breath exposure to the confined natural mercury vapor in permitted intake of 2 μg per each kg body weight per day [5]. Several sources have contributed significantly to mercury outflow into the environment like oil refineries, chloralkali wastewater, paper and pulp fabricating, power generation plants, fertilizers industries, rubber processing and comparable industry [6, 7].

Combustion of hydrocarbons was listed as anthropogenic sources of mercuric compounds to the environment in the world. A side from that, rivers polluted with mercury from liquid discharges, nearby petroleum refineries and petrochemical plants, where mercury is the most known and common heavy metals present in petroleum oil and natural gas [8]. An assortment of mercury-containing species, including elemental mercury, their compounds, and a mixture thereof, is contained in many types of crude oils [9]. The existence of these elements in crude oils can cause serious impacts because of their posing good product quality, environmental and safety issues. Besides, the effect of mercury present in feeds on processing systems which includes the deterioration of equipment components, catalyst poisoning, hazardous waste production, and an increased risk to workers' health and safety. All of these factors may cause reduction the final hydrocarbon product qualities, either directly or indirectly [10]. Mercury in some oil field, sources of water and refinery wastewater was of low concentrations, but still above the regulatory discharge limits. Mercury solubility is controlled by elemental mercury (~ 60 ppb at 25 °C). The oxidation of contaminated water leads to increasing of mercury concentration by solubility of elemental mercury by formation of ionic species. Removal of mercury present in water before discharge into the environment is generally minimize the effect of contamination and biotic methylation with mercury [11]. It is clear from the above considerations that removal of mercury from oil, water, industrial wastes and wastewater is a main target of most environmental researchers. Several techniques are accessible; ion exchange [12], adsorption [13], chemical precipitation [14], coagulation [15] and membrane technologies [16]. Adsorption is the most versatile and commonly used technique. The most widely sorbent used is activated carbon. Because of, activated carbon is costly, other sorbent materials are listed in the last years, especially of low-cost adsorbents [17–21].

However, most of used adsorbents endure from low adsorption capacities, in addition, low removal efficiencies of Hg (II). Consequently, researchers have been looking for new efficient adsorbents. Polymeric materials of polyfunctional groups are more prominent candidates as adsorbents due to their have high removal capacity and quick rate of adsorption [13, 22–25].

Styrene as one of the most flexible monomers available can be polymerized by different techniques such as free radical, anionic and cationic polymerization, group transfer, redox, thermal photopolymerization, and radiation polymerization. In addition, styrene can be polymerized using a variety of methods, suspension, emulsion, solution. The most widely used polymerization technique is the bulk polymerization. Each approach would result in a different set of product characteristics. Furthermore, acrylonitrile, butadiene, acrylates, vinyl acetate, vinylchloride, and a variety of other monomers can easily co-polymerize with styrene [26]. Acrylamide (AA) can be used as a co-monomer during the polymerization of styrene in an emulsifier and/or free aqueous medium. Because of the existence of amide groups structure surface, AA is supposed to act as a stabilizer for the resulting latex, allowing it to be used for a variety of purposes [27]. Conducting polymers such as polyanilines have been utilized in many fields including erosion assurance, auxiliary rechargeable batteries, sensors and controlled medicate conveyance [28–34]. Polyanilines (PANI) are a promising conducting polymer due to their price and different properties, stability, ease of synthesis and treatment. PANI and polyaniline/polystyrene composite have been utilized as the base material for the adsorption of Hg ions from aqueous media [35–38]. On amino group present in natural [24, 39, 40] and/or synthetic polymers was performed using aniline derivatives to check their properties in different applications [41–44].

The main target of this work is the uptake of Hg (II) from wastewater in petroleum field, based on easy and cheap polymeric materials. Styrene-acrylamide (14:1) copolymer was synthesized by emulsion polymerization technique in the presence of 4-dodecylbezenesulfonic acid and ammonium persulfate (APS) at 70 °C under nitrogen. The obtained copolymer was grafted with both polyaniline and poly (2-chloroaniline) using APS as oxidant in THF/water (1:1.5 v/v) at 5 °C. The prepared polymeric samples are dried and grinded for characterization and removal application of Hg (II) from wastewater in petroleum field. The data reveal that the grafting enhances the efficiency of acrylamide-styrene copolymer towards removal of Hg (II) > 99%. In addition, the

adsorption processes are obeyed Freundlich isotherm and pseudo-second-order kinetics.

2 Methods

2.1 Materials

Styrene ≥ 99%, dimethylformamide (DMF) 99%, ammonium persulfate (APS), and 4-dodecylbezenesulfonic acid (emulsifier) ≥ 95% were all purchased from Sigma-Aldrich (Germany). Acrylamide 98% and tetrahydrofuran (THF) 99.5% were products of Loba-Chemie (India). Aniline 99% and 2-chloroaniline 98% were produced from Merck-Co (Germany). Dithizone AR 99.1% was produced from Qualikems (India). Mercuric chloride (99%) was produced from Alpha Chemika (India). Sodium hydroxide pellets 98.5% and methanol 99.5% were provided by El-Nasr Pharmaceutical Chemical Company (Egypt). The water used in all experiments is distilled water.

2.2 Synthesis of styrene/acrylamide (14:1) copolymer

Styrene-co-acrylamide was synthesized by free emulsion polymerization in a three-necked flask equipped with a reflux condenser and a mechanical stirrer immersed in water bath as follows [45].

Fourteen milliliters styrene was miscible in 20 mL DMF in a closed flask in the presence of 0.2 mL of 4-dodecylbezenesulfonic acid. In a second flask 0.7108 g acrylamide was dissolved in 10 mL distilled water. In a third flask 5 g APS was dissolved in 10 mL distilled water. The three flasks were left 10 min in a 60 °C water bath. Then, acrylamide solution was poured slowly on styrene solution with manual stirring. After that, APS as initiator was slowly added to the reaction flask containing two monomers with reflux and stirring (400 revolutions per minute (rpm)) at 60 °C for 3 h, and then, the reaction left at room temperature overnight. The copolymer was isolated

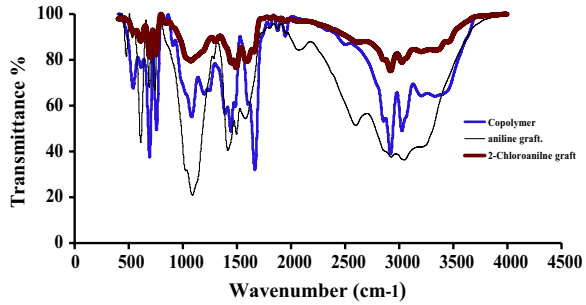

Fig. 1 IR spectrum of the investigated polymeric samples

Table 1 IR absorption bands and their assignments

Wave number			Assignment	References
Copolymer	Aniline graft	2-Chloroaniline graft		
		$3454^{S/B}$	NH_2 stretching	[47]
$3332^{S/B}$		$3332^{S/B}$		
$3205^{S/M\,B}$	$3200^{S/B}$	$3202^{S/M\,B}$	H-bonded NH Stretching	[48–51]
3026^{S}	$3049^{S/B}$	3026^{S}	Aromatic C–H stretching/H-bonded (N–H)	[52–54]
2921^{S}	2926^{S}	2921^{S}	Aliphatic CH stretching	[55]
2857^{M}		2859^{S}		
2503^{W}	2600^{S}	$2618^{M/B}$		
1668^{S}		$1659^{S/M}$	C=O	[56]
$1604^{SH/Sh}$	$1578^{M/B}$	1593^{S}		
1445^{S}	1418^{S}	1448^{S}	C–N stretching/C=C stretching of benzene ring	[52, 53]
1394^{S}	1288^{W}	1303^{M}	CH_2 bending	[57]
1248^{M}				
1199^{M}				
$1083^{S/B}$	1090^{B}	$1074^{S/B}$	In plan deformation (CH) (mono substituted ring)	[52, 53, 58]
$758^{S/SH}$	742^{M}	753^{S}	Out of plan NH bend/out-of-plan deformation CH (mono substituted or 1,2-di substituted ring)	[48, 52–54, 57–59]
$694^{S/SH}$	691^{M}	694^{S}	Out of plan NH bend/out-of-plan ring bending (mono substituted ring) and/or aryl C–Cl stretching vibration	[52–54, 57, 59, 60]
615^{W}	$612^{S/SH}$	$612^{M/SH}$		

S, Strong; B, Broad; M, Medium; W, Weak; SH, Sharp; Sh, Shoulder

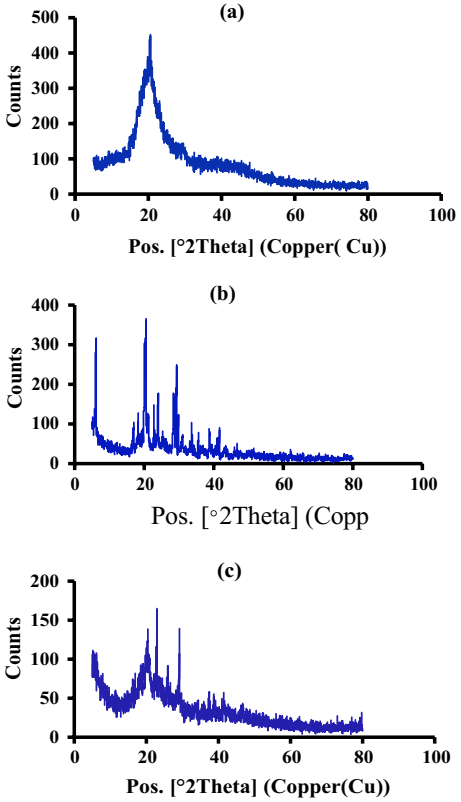

Fig. 2 XRD pattern of copolymer (**a**), aniline graft (**b**) and 2-chloroaniline graft (**c**)

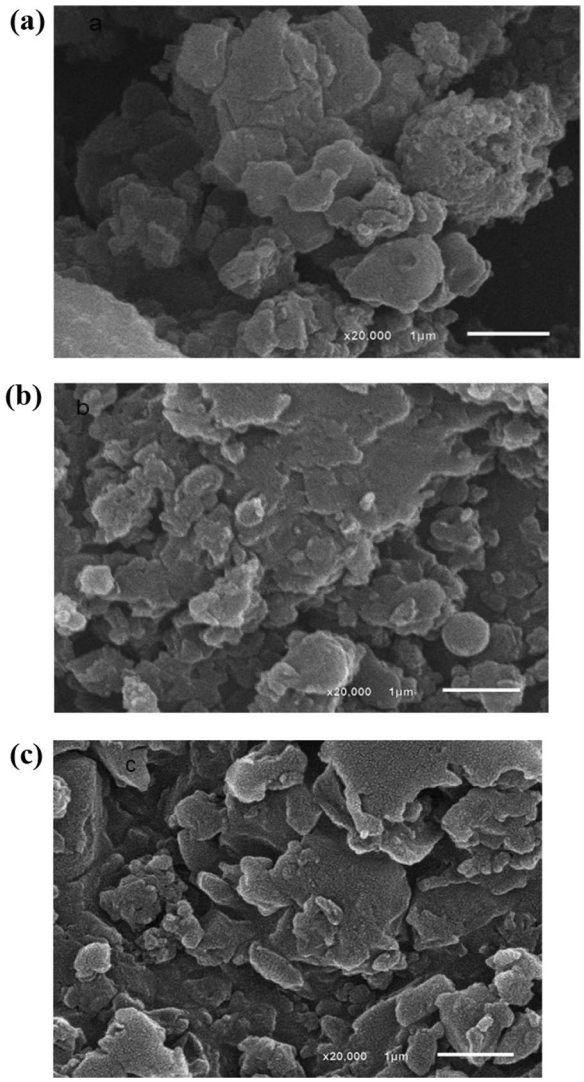

Fig. 3 SEM images of styrene-acrylamide (14:1) copolymer (**a**), aniline graft (**b**) and 2-chloroaniline graft (**c**)

by addition of 20 mL methanol as non-solvent and then washed with both distilled water and DMF, and dried in vacuum oven at 60 °C.

2.3 Synthesis of styrene-co-acrylamide-gr-aniline and 2-chloroaniline in general

Styrene-co-acrylamide (0.5 g) was dissolved in 10 mL THF, and 1 mL of aniline or 2-chloroaniline was dissolved in the copolymer solution by stirring during the addition. APS solution (0.5 g/15 mL) was added to the reaction medium thermostated at 5 °C under nitrogen for 3 h. After that, the polymerization reaction was left overnight. The formed graft was collected by decantation and continuous washing with DMF/water (1:1) mixture and then dried at room temperature and finally in vacuum oven at 70 °C [43, 44].

2.4 Instrumental techniques

The infrared measurements were carried out using Shimadzu FTIR Vertex 70 Bruker Optics (Japan) technique to identify the functional groups for both synthesized copolymer and their grafts. Fourier transform infrared (FTIR) spectra of the samples were recorded from 400 to 4000 cm^{-1} using KBr pellets at room temperature.

2.5 Ultraviolet visible spectroscopy

Ultraviolet spectroscopy of investigated materials is carried out using Shimadzu visible spectrophotometer Double beam 2600. Also, Hg (II) solution was followed and measured spectrophotometrically at 520 nm.

2.6 Morphological studies using XRD and SEM

The XRD patterns of synthesized copolymer and its grafts were characterized using PANalytical Empyrean

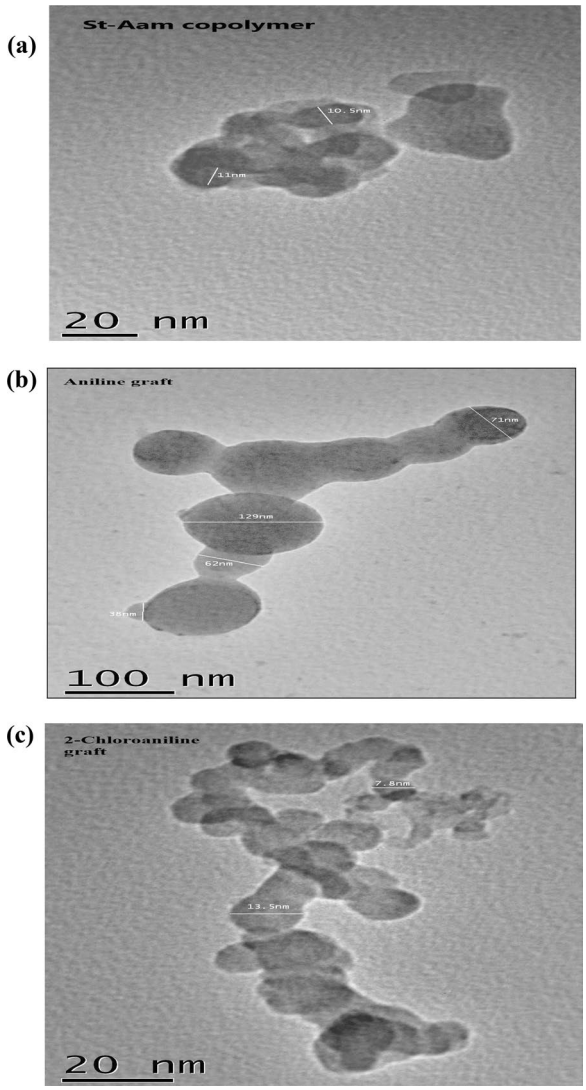

Fig. 4 TEM images of **a** copolymer, **b** aniline graft and **c** 2-chloroaniline graft

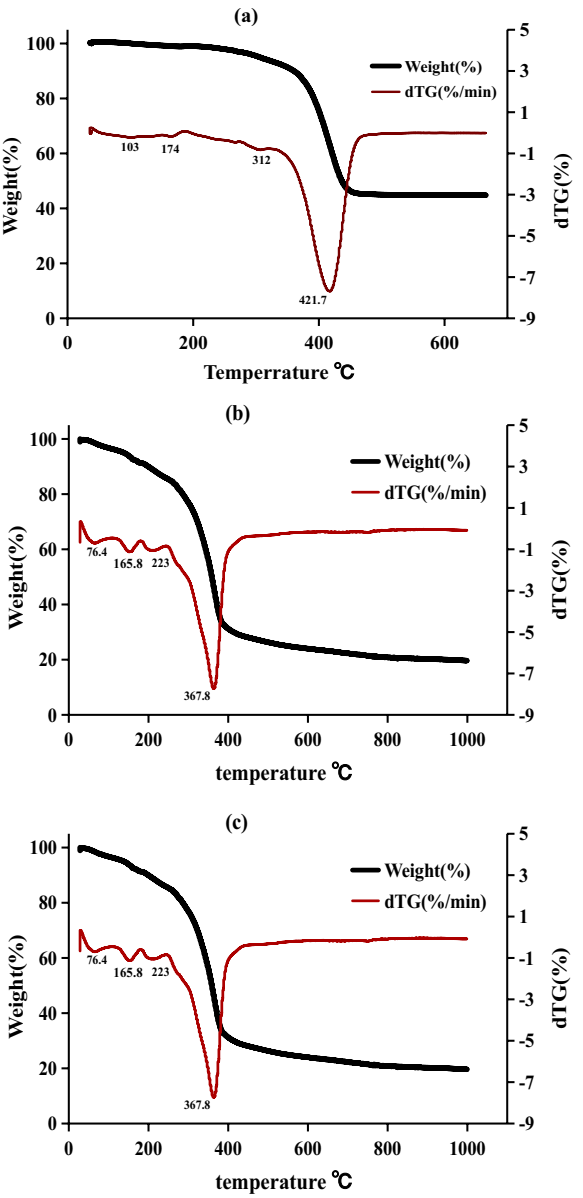

Fig. 5 TGA of copolymer (**a**), aniline graft (**b**) and 2-chloroaniline graft (**c**)

X-ray diffractometer 202964. The scan range was (5°–140°).

The electron microscopic pictures were taken using JSM-6510LA scanning electron microscopy (SEM), JEOL, Japan. TEM measurements were carried out using a carbon-coated copper grid as a photographic plate of the transmission electron microscope.

2.7 Thermogravimetric analysis

Thermogravimetric analysis (TGA) analysis using detector type Shimadzu TGA-50H with its component platinum cell, nitrogen atmosphere, and 20 °C/min rate flowing was used to investigate the thermal stability of the prepared polymeric samples.

2.8 BET measurements

The nitrogen adsorption–desorption measurements of the polymeric samples were performed using BELSORP-max Ver1.3.5 analyzer. The specific surface areas were determined based on Brunauer–Emmett–Teller (BET) theory. Pore size distributions were deduced from the adsorption isotherms according to the nonlocal density function theory (NLDFT).

Table 2 TGA data of the synthesized polymeric samples

Copolymer		Aniline graft		2-Chloroaniline graft		Assignments
Mid-point °C	Approx. wt loss%	Mid-point °C	Approx. wt loss%	Mid-point °C	Approx. wt loss%	
103	0.06	≤100	0.045	≤100	2.4	Humidity loss
174	1.04	–	–	166	5.4	Bonded water loss
–	–	202	8.56	–	–	
–	–	227	5.4	223	4.75	Doping counter ions losing on amine and/or imine nitrogen atom in case of benzenoid or quinoid rings
312	4.6	–	–	–	–	May be attributed to losing of aliphatic part of copolymer
421.7	34.0	318.1	15.99	368	44.05	
–	–	420	26.0			
–	–	812	9.0	–	–	
>421.7	60.3	>812	35.0	>368	43.4	Carbon residues

2.9 Adsorption studies

The contaminated samples with mercuric were supplied from the Egyptian petroleum research institute (EPRI) [8]. In general, Hg^{2+} concentration was followed by measuring the absorbance of Hg (II)/dithizone (dissolved in isopropyl alcohol) [46] purple color at 520 nm, using ultraviolet spectroscopy carried out using Shimadzu visible spectrophotometer Double beam 2600. The mercury loading capacities were calculated from the initial and final Hg (II) contents of the solution.

3 Results

3.1 Characterization of polymeric samples

3.1.1 IR spectrum and UV–visible spectroscopy

Infrared spectrums of styrene-co-acrylamide and their polyaniline and poly (2-chloroaniline) grafts are represented in Fig. 1, and the absorption bands are given in Table 1. The other absorptions and their matching are summarized in Table 1.

The UV–visible spectroscopy of the three prepared polymeric samples reveals that the maximum absorption bands are at 393, 544 and 546 nm for copolymer, copolymer/aniline and copolymer/2-chloroaniline graft, respectively. The intensities of graft peaks are very high with respect to the copolymer one which indicated the difference in structures and electronic transition. This difference may be due to differences in charges densities of π-electrons and structures on the present polymeric samples.

3.1.2 XRD, SEM and TEM

XRD patterns of the prepared polymeric samples are presented in Fig. 2. The figure shows that the grafting process of both aniline and 2-chloroaniline into styrene/acrylamide copolymer enhanced the crystallinity of copolymer. In addition, the crystallite size (nm) is changed, and for copolymer, there are only two sizes 5.58 and 11.00. In case of copolymer grafted with aniline, the crystallite size ranged from 5.25 to 93.23 with more than one size and in case of grafting with 2-chloroaniline the crystallite size decrease with variation in size to be 1.28–93.12.

Scan electron microscope (SEM) and transmission electron microscope (TEM) pictures for the three polymeric materials are given in Figs. 3 and 4. The pictures show that the grafting process gives variation in particle shapes and sizes. Surface with internal voids and particles of irregular shapes and broad size distribution also, hollow spheres are observed. Grafts include spherical particle shapes more than copolymer. In addition, the size of particles is 10.5–11 nm in case of copolymer which increased on grafting with polyaniline and ranged from 38 to 129 nm, but the grafting with 2-chloroaniline the particle size decreased and ranged from 7.8 to 13 nm.

3.1.3 Thermogravimetric analysis (TGA)

The effect of temperature on the weight of polymeric samples under investigation is presented in Fig. 5. The weight loss of polymeric samples was followed with raising temperature up to ~ 1000 °C except in copolymer up to 700 °C due to thermal stability of the residual carbonic matter. The thermal fragmentation of investigated polymeric samples and their assignment are summarized in Table 2.

3.1.4 BET measurements

The adsorption–desorption of N_2 gas on the surface of the three polymeric samples is followed in the range of p/p^o 0–100. The data are presented in Fig. 6. The figure reveals that the adsorption on these surfaces is of Type III, which indicates unrestricted multi-layer formation process with strong interaction between adsorbate and

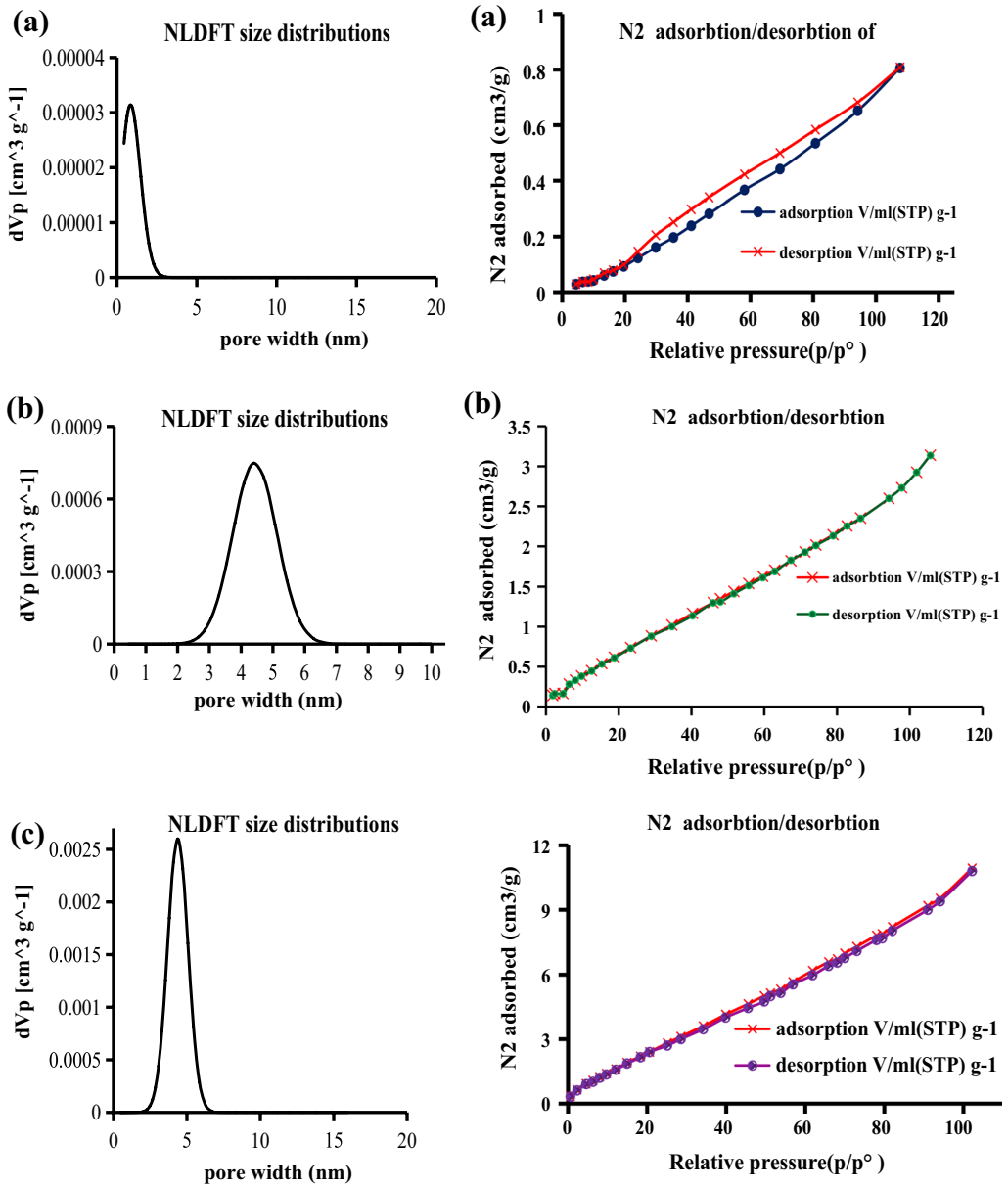

Fig. 6 BET graphs of copolymer, aniline graft and 2-chloroaniline graft

synthetic polymeric adsorbents. In addition, the hysteresis loop like H_4 loop gives narrow slit-like pore, and there are internal voids, particles of irregular shapes, broad size distribution and hollow spheres with wall composed of ordered mesopores surfaces which agreed with both SEM and TEM pictures. The relation between d*V*p [$cm^3\ g^{-1}$] against pore width (nm) is also presented in Fig. 6. The measured data are given in Table 3. The data reveal that the grafting process enhances these variables of copolymer, such as surface area and pore size.

3.2 Adsorption of Hg (II) onto copolymer and their grafts

3.2.1 Influence of contact time using different doses of polymeric sorbents

Effect of contact time on removal % of Hg (II) in the presence of styrene-acrylamide (14:1) copolymer, aniline graft and 2-Chloroaniline graft copolymers as new sorbents with polymer weights of (0.1, 0.2, 0.3 and 0.5 g) were separately studied. The obtained data are graphically presented in Fig. 7. Data reveal that, the ability of the polymeric sorbents on the removal of Hg (II) increases by increasing both copolymer weight and

Table 3 Pore size and surface area parameters of the polymer samples

Variables	Copolymer	Aniline graft	2-Chloroaniline graft
Pore size. V_p (cm^3/g)	0.0005	0.0042	0.0149
W_1 (peak area) nm	0.4422	4.3903	4.3903
W_2 (peak volume) nm	0.7305	4.3903	4.3903
V_m cm^3/g (stp)	0.3227	0.9580	3.3586
Total pore volume cm^3/g	0.0012	0.0049	0.0169
C	1.3857	5.5895	5.9617
Mean pore diameter nm	3.5114	4.6581	4.6278
Surface area m^2/g	1.4045	4.1698	14.6180

contact time in the range of study. All experiments were performed at pH = 7 and 20 °C. At 20 min the removal efficacy % of copolymer, aniline graft and 2-chloroaniline graft are 65, 96.3 and 99.7, respectively, using 0.5 g of sorbents. Also, the efficiency of grafts becomes good at 0.2 g sorbents and then increased by increasing the quantity of dose due to increasing of polymer surface areas and functions by increasing their quantities.

3.2.2 Effect of temperature and thermodynamics

The effect of temperature in the range 15–37 °C on Hg (II) uptake from petroleum source using 0.5 g of each investigated polymeric samples was separately performed at pH = 7. The obtained data with time are graphically presented in Fig. 8. The results of the three polymer samples show that removal efficiency decreases with raising temperature. The thermodynamic parameters can be deduced from the relations [61].

$$\Delta G^{\circ} = -RT \operatorname{Ln} K_c \tag{1}$$

$$\Delta G^{\circ} = \Delta H^{\circ} - T\Delta S^{\circ} \tag{2}$$

$$\operatorname{Ln} K_c = \Delta S^{\circ}/R + \Delta H^{\circ}/RT \tag{3}$$

where R is the universal gas constant (8.314 J mol^{-1} K^{-1}), T is the temperature in Kelvin, ($\Delta H°$) is the standard enthalpy, K_C is the Langmuir constant, and ($\Delta S°$) is the entropy of the adsorption process. Both $\Delta H°$ and $\Delta S°$ of adsorption are estimated from the relationship between $\ln K_C$ versus $1/T$ (cf. Fig. 9) [62]. The calculated data are tabulated in Table 4. The calculated data were performed at time 20, 15 and 5 min for copolymer, aniline graft and 2-chloroaniline graft, respectively.

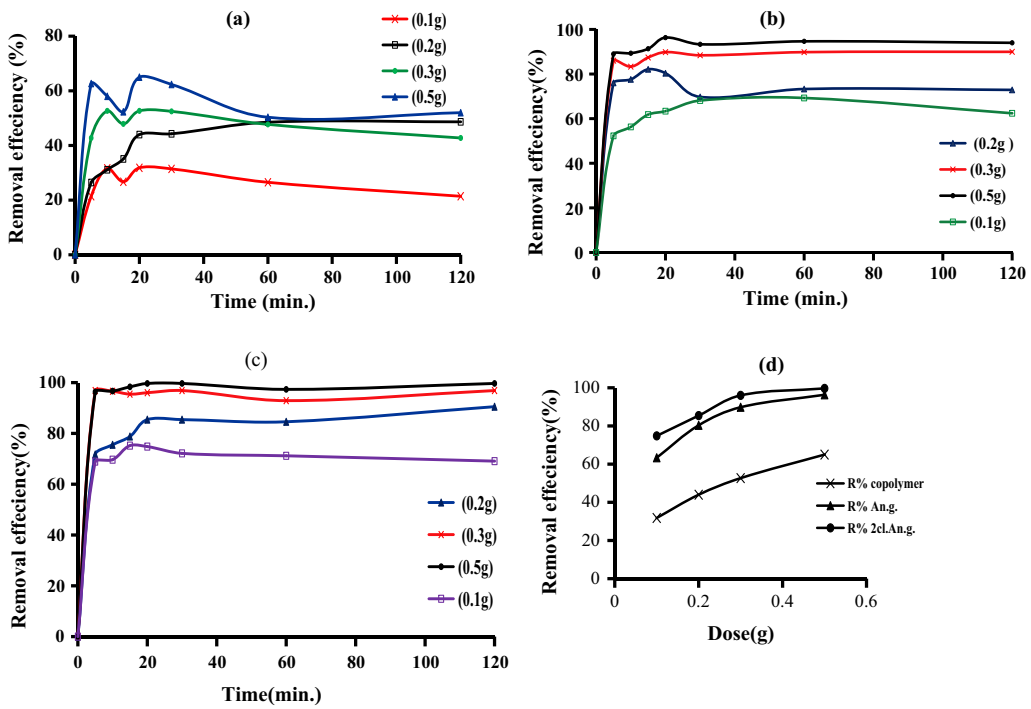

Fig. 7 Removal efficiency (%) of copolymer (**a**), aniline graft (**b**) and 2-chloroaniline graft (**c**) doses at different time intervals at contact time 20 m for three samples (**d**)

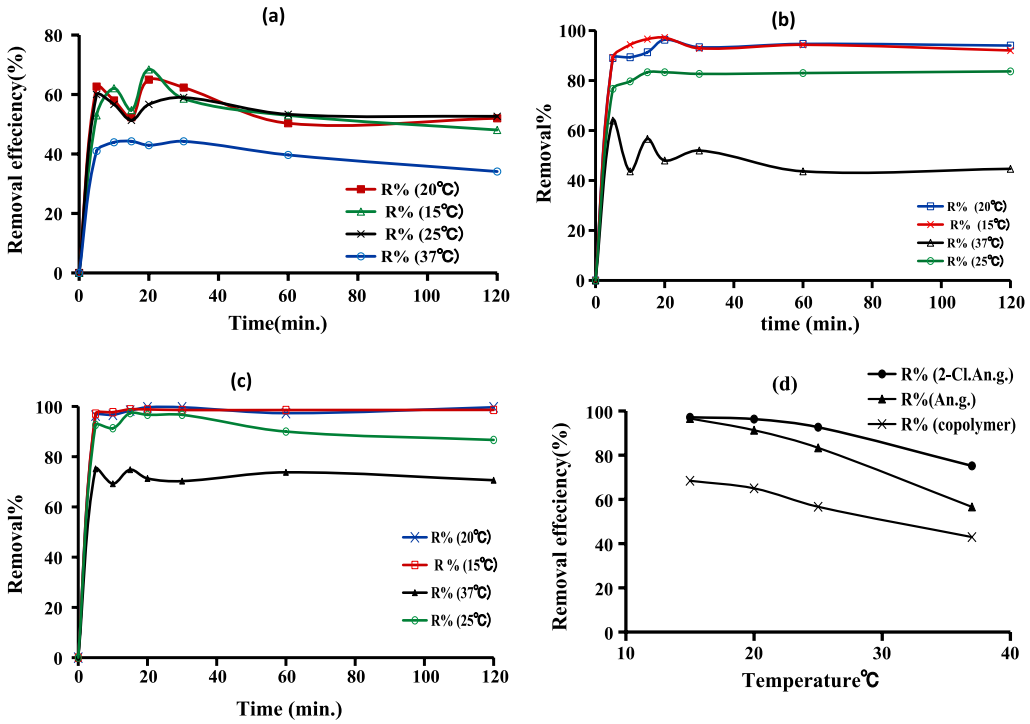

Fig. 8 Removal efficiency (%) of copolymer (**a**), aniline graft (**b**) and 2-chloroaniline graft (**c**) and with time contacts 20 m, 15 m and 5 m (**d**) at temperatures 15 °C, 20 °C, 25 °C and 37 °C

The values of the standard enthalpy (ΔH°) in Table 4, reveal that the adsorption of Hg^{2+} on the surface of the three polymer materials is endothermic. The negative value of Gibbs free energy refer to the adsorption process is spontaneous.

3.3 Adsorption isotherms

3.3.1 Langmuir isotherm

The formation of mono-layer adsorbate on the surface of adsorbent, which describes quantitatively, then no addition of any adsorption layers takes place, hence Langmuir model illustrate the equilibrium distribution of metal ions between solid and liquid phase. Langmuir represented Eq. (4), [63].

$$C_e/q_e = C_e/Q_m + 1/Q_m b \quad (4)$$

where

C_e is the equilibrium concentration of adsorbate (mg L^{-1}).

q_e is the amount of Hg^{+2} adsorbed per gram of the adsorbent at equilibrium (mg g^{-1}).

Q_m is maximum mono-layer coverage capacity (mg g^{-1}).

K_L is Langmuir isotherm constant (L mg^{-1}).

The values of Q_m and K_L were calculated from the slope and intercept of plot C_e/q_e versus C_e, (see Fig. 10).

3.3.2 Freundlich isotherm

The widely applied isotherm in the investigation of adsorption of different compounds on solid surfaces is Freundlich isotherm [64]. In the present work, Freundlich model is used to investigate the adsorption results of Hg^{2+} on copolymer, aniline graft and 2-chloroaniline graft, the equilibrium results are fitted with the logarithmic form of Freundlich model. Nonlinear form of Freundlich adsorption model is $q_e = K_f C_e^{1/n}$, but the linear form is presented in Eq. (5). The equilibrium concentration of adsorbed metal ion on solid copolymer surface is expressed by q_e (mg/g), C_e is bulk concentrations of metal ion at equilibrium (mg/L), K_f is isotherm constant and n refers to adsorption intensity.

K_f is an indicator of adsorption capacity, while $1/n$ refers to the adsorption strength in the process which

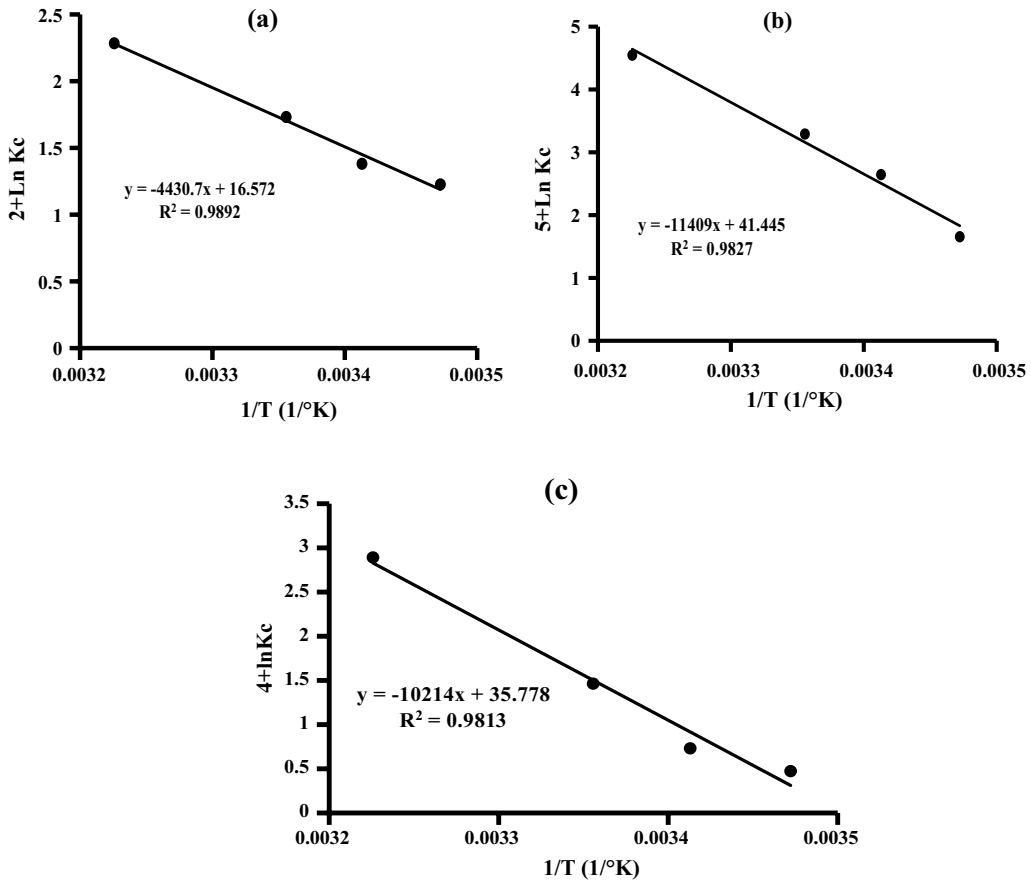

Fig. 9 Van't Hoff plot for the adsorption of Hg^{2+} on copolymer (**a**), aniline graft (**b**) and 2-chloroniline graft (**c**)

Table 4 Thermodynamic parameters

Temperature (K)	Δ*G* (kJ/Mole)		
	Copolymer	Aniline graft	2-Chloroaniline graft
288	− 1.85	− 8.01	− 8.44
293	− 1.51	− 5.74	− 7.96
298	− 0.66	− 4.23	− 6.28
310	0.73	− 1.17	− 2.86
Δ*H* (kJ mol^{-1})	36.83	94.85	84.92
Δ*S* (J mol^{-1} K^{-1})	137.78	344.53	297.45

deduced form the intercept and the slope of linear Freundlich form, (see Fig. 11).

$$\text{Ln}\, q_e = \text{Ln}\, K_f + (1/n)\, \text{Ln}\, C_e \quad (5)$$

3.3.3 Temkin isotherm

Temkin isotherm model [65] contains factor refer to the interaction between adsorbates which absent in case of Langmuir isotherm model. Thermodynamic data reflected the endothermic nature for adsorption of mercury ion using copolymer. The adsorbent–adsorbate interactions are governed by factors present in Temkin isotherm. By ignoring the concentration values of all molecules in the layer, adsorption decreases linearly rather than logarithmic with coverage.

$$q_e = B_T \text{Ln}\, K_T + B_T \text{Ln}\, C_e \quad (6)$$

where q_e is the amount of adsorbed Hg^{2+} by the polymeric sample at equilibrium (mg g^{-1}), B_T is constant and equal to RT/*b* that related to the heat of sorption (J mol^{-1}), and *R* is the general gas constant (8.314 J mol^{-1}), *T* is the temperature in Kelvin (K), *b* is Temkin isotherm constant, and K_T is the Temkin isotherm equilibrium binding constant (L g^{-1}). The plots of $\ln q_e$ versus $\ln C_e$ (see Fig. 12). The adsorption data obtained for the three investigated polymeric samples are summarized in Table 5.

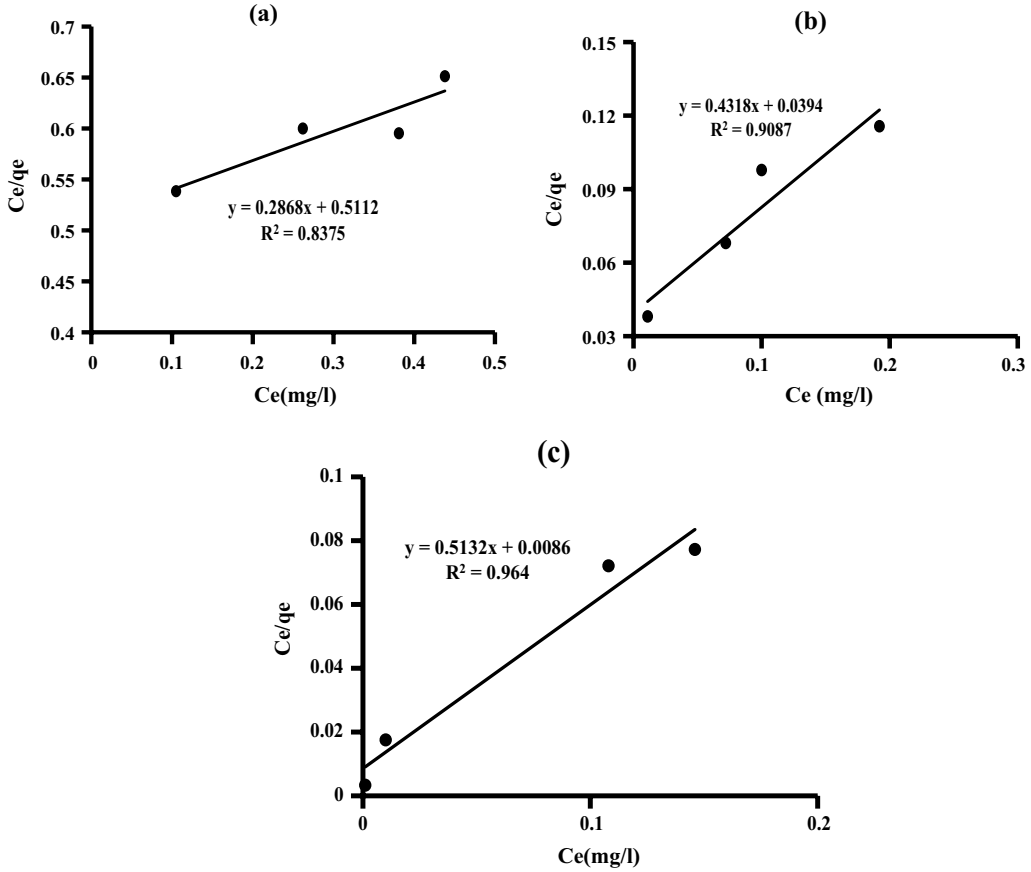

Fig. 10 Langmuir isotherm of copolymer (**a**), aniline graft (**b**) and 2-chloroaniline graft (**c**)

3.4 Adsorption kinetics

Kinetic adsorption studies of mercuric ion on styrene-acrylamide (14:1), aniline graft and 2-chloroaniline graft copolymers were investigated to evaluate the rate/order of adsorption. Order of adsorption is analyzed using two kinetic models called pseudo-first-order kinetic model [66] that presents the relations between rate of sorption sites for the adsorbents which occupied and the unoccupied sites (Eq. 7), and pseudo-second-order kinetic model [67] which shows the dependency of adsorbent capacity for adsorption on time (Eq. 8).

$$\mathrm{Ln}\,(q_e - q_t) = \mathrm{Ln}\,q_e - K_1 t \tag{7}$$

$$\mathrm{t/qt} = 1/\mathrm{k_2 q_e^2} + \mathrm{t/q_e} \tag{8}$$

where k_1 (min^{-1}) is the rate constant of the pseudo-first order, both q_e and q_t are the amount of metal ion adsorbed (mg/g) at equilibrium and at time t (min) and k_2 is the rate constant of pseudo-second order (g mg^{-1} min^{-1}). The graphical representation of the two models is given in Figs. 13 and 14. Parameters of the first and second-order models were deduced from the slope and intercept of linear relations of both ln (q_e–q_t) versus t and (t/q_t) versus t (see Figs. 13 and 14). The obtained data are given in Table 6.

From the obtained data presented in Figs. 13 and 14, Table 6 and the values of R^2, it is clear that the sorption process of Hg^{+2} on the surface of styrene-acrylamide (14:1), aniline graft and 2-chloroaniline graft copolymers is proceed via the Lagergren pseudo-second order reaction.

4 Discussion

4.1 Characterization of investigated polymeric samples

The obtained results reveal that the grafting of both polyaniline and poly (2-chloroaniline) on styrene-co-acrylamide was achieved. This fact can be confirmed as follows:

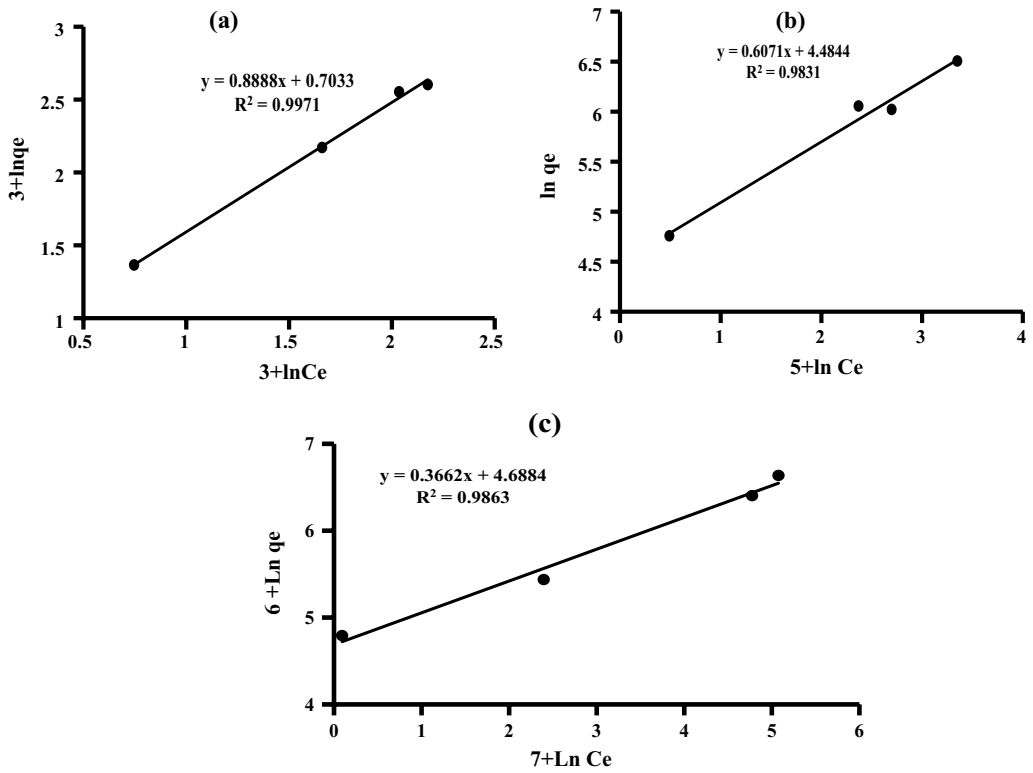

Fig. 11 Freundlich isotherm of copolymer (**a**), aniline graft (**b**) and 2-chloroaniline graft (**c**)

From both Fig. 1 and Table 1, it is clear that the stretching vibration band intensities of free amino groups present in copolymer structure are reduced by grafting which indicates the performance of grafting process [40]. The grafting process enhances the crystallinity of copolymer and gives more wide range of crystallite sizes. That is clear from XRD patterns. The observed difference in shapes and particle size in SEM and TEM pictures, indicates the difference in morphology between the three prepared polymeric samples. From Fig. 5 (TGA) and Table 2, it can be concluded that the temperature of degradation (Td) is 421.7, 318 and 368 for copolymer, aniline graft and 2-chloroaniline graft, respectively, which means the grafting lowering Td. BET measurements reveal the differences between pore size and surface area between the three investigated polymeric materials which also confirm the suggested synthetic copolymer and its graft.

4.2 Adsorption of Hg (II)

The adsorption of Hg (II) results can be rationalized by the increasing of active sites of polymeric surface by increasing their weights. In addition, the sorption process proceeds to completion on time. At 20 min contact time the removal % efficacy of copolymer, aniline graft and 2-chloroaniline graft are 65, 96.3 and 99.7, respectively, using 0.5 g of sorbents (cf. Fig. 7). Also, the efficiency of grafts becomes good at 0.2 g sorbents then increased by increasing the quantity of dose. That means the grafting process of styrene-acrylamide (14–1) copolymer with polyaniline and poly (2-chloroaniline) enhances the efficiency of copolymer on Hg (II) uptake. Which can be attributed to the increasing of active groups (such as –NH–, $-NH_2$, –Cl), surface area and pore sizes. The moieties of both polyaniline and poly (2-chloroaniline) contain the above-mentioned function groups, so on grafting these groups increase in the used polymer samples which leads to enhancement efficiencies. The adsorption of Hg (II) in our study decreases with rising temperature and the process is endothermic (+ ve values of ΔH) and spontaneous occurring (ΔG −ve values) (cf. Fig. 8). It is clear from the data of three investigated isotherms that the adsorption of Hg (II) on the surface of these polymeric samples are multi-layers obeying Freundlich isotherm. This result confirms the obtained morphology by BET measurements. In addition, kinetic data confirm the

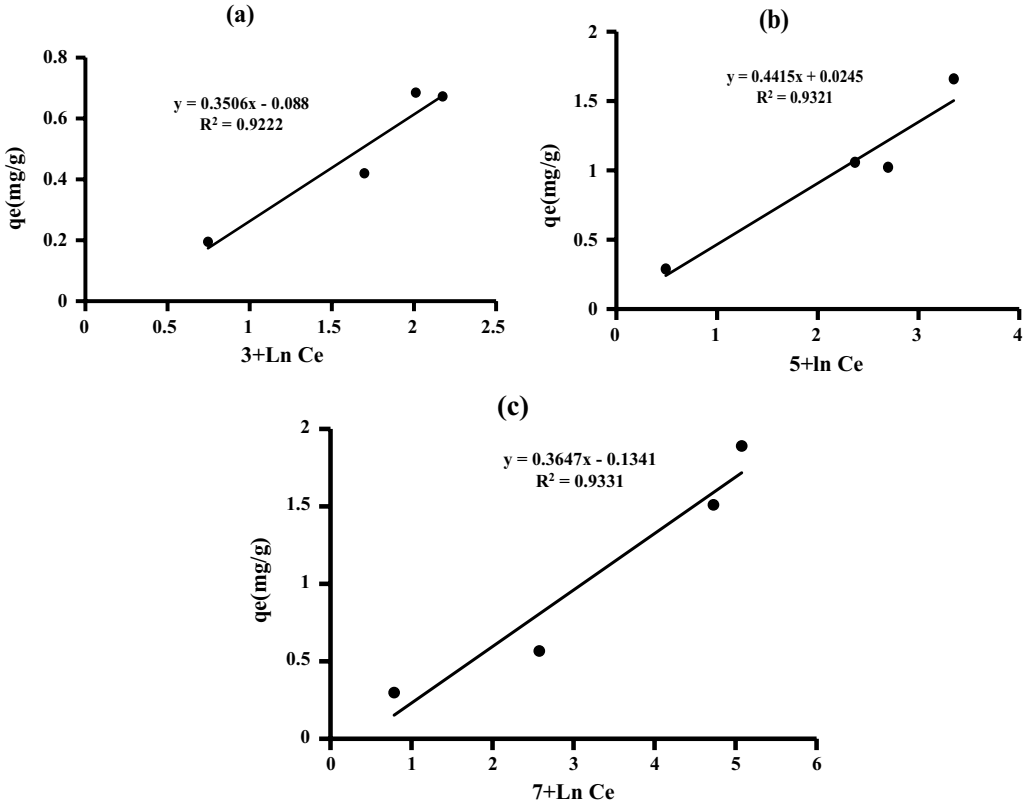

Fig. 12 Temkin isotherm of copolymer (**a**), aniline graft (**b**) and 2-chloroaniline graft (**c**)

Table 5 Isothermic parameters for the adsorption of Hg^{2+} on polymer samples

Model	Isothermic parameters	Parameter values		
		Copolymer	Aniline graft	2-Chloroaniline graft
Langmuir	Q_m (mg g^{-1})	3.48	2.31	1.95
	B	0.511	10.96	59.67
	R^2	0.83	0.908	0.964
Freundlich	N	0.83	1.64	2.73
	K_f (mg g^{-1})	2.02	88.62	108.68
	R^2	0.997	0.983	0.986
Temkin	B_T (J mol^{-1})	0.350	0.442	0.364
	K_T (L g^{-1})	1.072	1.057	0.692
	R^2	0.922	0.932	0.933

Lagergren pseudo-second order reaction (cf. Figs. 13, 14). This confirms the removal mechanism by both adsorption and complex formation of Hg (II) with both unpaired and π electrons present in copolymer structure on –NH–, $–NH_2$, –Cl and benzene or quinoid units, respectively. In addition, it can discuss the chemical adsorption type which can occurs by interaction between the used polymeric adsorbent materials and the dissolved mercuric ions beside the physical one [60].

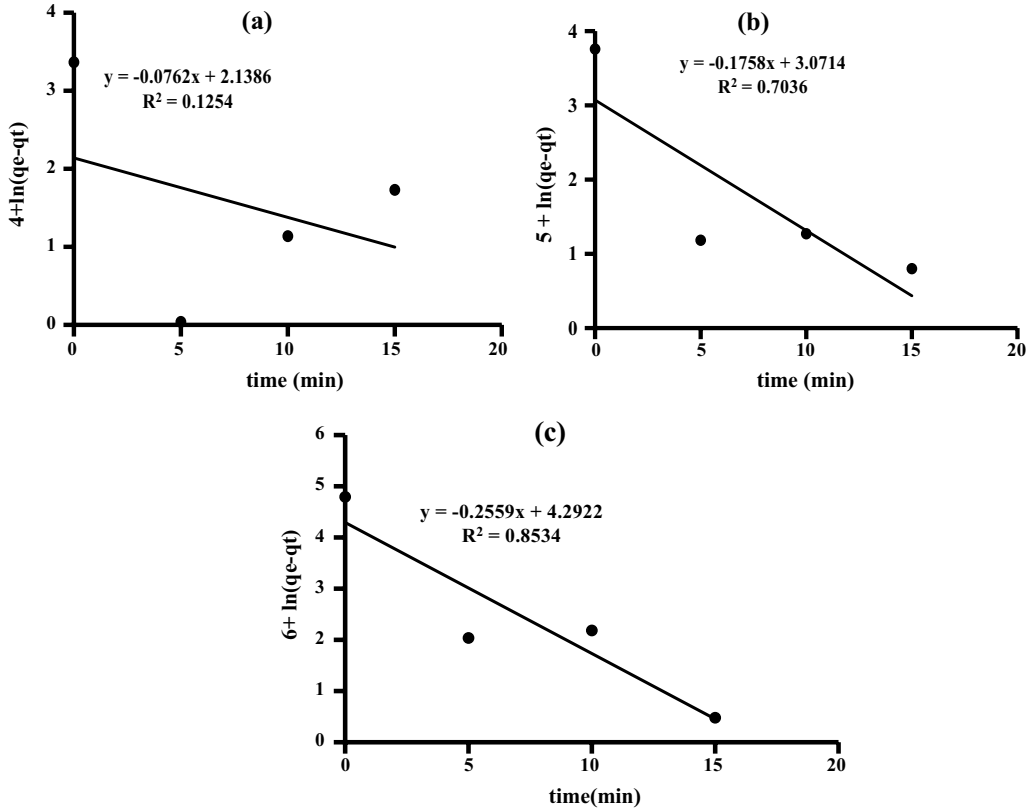

Fig. 13 First-order module of copolymer (**a**), aniline graft (**b**) and 2-chloroaniline graft (**c**)

Table 6 Kinetic models data

Model	Parameter	Parameter value		
		Copolymer	Aniline Graft	2-Chloroaniline graft
Pseudo first order	K_1 (min^{-1})	0.076	0.176	0.256
	q_e (mg g^{-1})	8.48	21.57	73.12
	R^2	0.125	0.704	0.853
Pseudo second order	K_2 (min^{-1})	1.82	14.63	6.91
	q_e (mg g^{-1})	0.148	0.283	0.298
	R^2	0.9914	0.9999	0.9994

5 Conclusions

In conclusion, styrene-acrylamide (14:1) copolymer was synthesized simply using free emulsion polymerization technique, and then, it was used as a base for synthesize of aniline and 2-chloroaniline graft copolymers. The polymer samples were characterized by FTIR, SEM, TEM, XRD, BET, and TGA; these prepared polymers are environmentally safe. Aniline and 2-chloroaniline grafts are found to have high removal efficacy for Hg^{2+}, while styrene-acrylamide copolymer has moderate one.

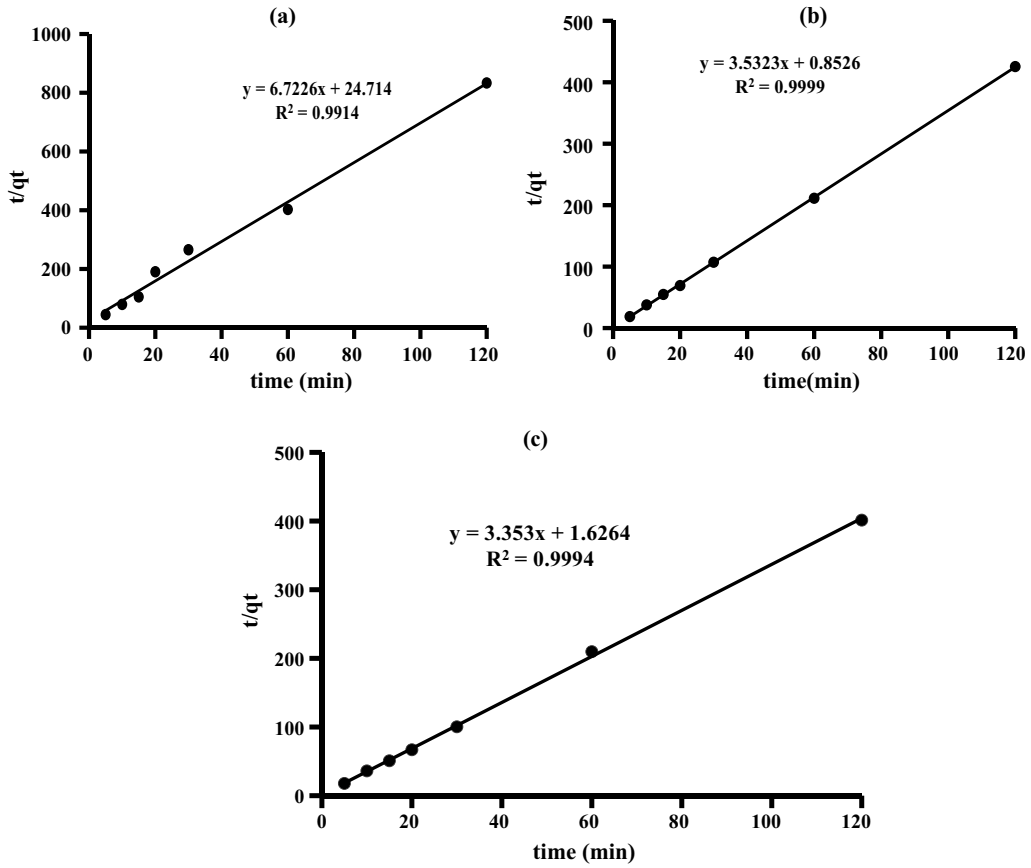

Fig. 14 Second-order module of copolymer (**a**), aniline graft (**b**) and 2-chloroaniline graft (**c**)

Acknowledgements
The authors thank Chemistry Department, Faculty of Science, Beni-Suef University, Egypt, for helping and continued supporting.

Author contributions
HMMF response on experimental data and typing process, EMSA response on some sampling and revision of paper, and HMAE-S response on suggesting idea work and interpretation of results. All authors read and approved the final manuscript.

Funding
There is no funding source else authors.

Availability of data and material
The data and materials of this research are available at authors laboratory.

Declarations

Ethics approval and consent to participate
Not applicable.

Consent for publication
Not applicable.

Competing interests
The authors declare that they have no known competing financial interests or personal relationships that could have appeared to influence the work reported in this paper.

Author details
[1]Department of Chemistry, Faculty of Science, Polymer Research Laboratory, Beni-Suef University, Beni-Suef City 62514, Egypt. [2]Petrochemicals Department, Egyptian Petroleum Research Institute, Nasr City 11727, Cairo, Egypt. [3]Department of Chemistry, College of Sciences, University of Ha'il, Hai'l 81451, Saudi Arabia.

Received: 25 January 2022 Accepted: 31 March 2022
Published online: 15 April 2022

References

1. Li Z, Wu L, Liu H, Lan H, Qu J (2013) Improvement of aqueous mercury adsorption on activated coke by thiol-functionalization. Chem Eng J 228:925–934
2. Risher JF, Amler SN (2005) Mercury exposure: evaluation and intervention the inappropriate use of chelating agents in the diagnosis and treatment of putative mercury poisoning. Neurotoxicology 26:691–699
3. Bose-O Reilly S, McCarty KM, Steckling N, Lettmeier B (2010) Mercury exposure and children's health. Curr Probl Pediatr Adolesc Health Care 40:186–215
4. Sondreal EA, Benson SA, Pavlish JH, Ralston NVC (2004) An overview of air quality III: mercury, trace elements, and particulate matter. Fuel Process Technol 85:425–440
5. Miretzkya P, Cirelli AF (2009) Hg (II) removal from water by chitosan and chitosan derivatives: a review. J Hazard Mater 167:10–23

6. Kim BJ, Bae KM, An KH, Park SJ (2011) Elemental mercury adsorption behaviors of chemically modified activated carbons. Bull Korean Chem Soc 32(4):1321–1326
7. Yardim MF, Budinova T, Ekinci E, Petrov N, Razvigorova M, Minkova V (2003) Removal of mercury (II) from aqueous solution by activated carbon obtained from furfural. Chemosphere 52(5):835–841
8. Mohamed FE, Gajdosechova Z, Masod MB, Zaki T, Feldmann J, Krupp EM (2016) Mercury speciation and distribution in an Egyptian natural gas processing plant. Energy Fuels 30(12):10236–10243
9. Granite EJ, Pennline HW, Hargis RA (2000) Novel sorbents for mercury removal from flue gas. Ind Eng Chem Res 39:1020–1029
10. Wilhelm SM, Liang L, Kirchgessner D (2006) Identification and properties of mercury species in crude oil. Energy Fuel 20:180–186
11. Gallup DL (2014) Removal of mercury from water in the petroleum industry. In: 21st annual international petroleum environmental conference, Houston, TX
12. Chiarle S, Ratto M, Rovatti M (2000) Mercury removal from water by ion exchange resins adsorption. Water Res 34(11):2971–2978
13. Rabee MM, Abd El-Salam HM (2022) Mercuric (II) up-taking from industrial wastewater based on poly(aniline-co-N-(2-hydroxyethyl)aniline as new sorbent. Polym Bull. https://doi.org/10.1007/s00289-021-04045-6
14. Blue LY, Jana P, Atwood DA (2010) Aqueous mercury precipitation with the synthetic dithiolate, BDTH2. Fuel 89(6):1326–1330
15. Lu X, Huangfu X, Ma J (2014) Removal of trace mercury (II) from aqueous solution by in situ formed Mn–Fe (hydr) oxides. J Hazard Mater 280:71–78
16. Bessbousse H, Rhlalou T, Verchère JF, Lebrun L (2010) Mercury removal from wastewater using a poly (vinylalcohol)/poly (vinylimidazole) complexing membrane. Chem Eng J 164(1):37–48
17. Dillon EC Jr, Wilton JH, Barlow JC, Watson WA (1989) Large surface area activated charcoal and the inhibition of aspirin absorption. Ann Emerg Med 18(5):547–552
18. Chada N, Romanos J, Hilton R, Suppes G, Burress J, Pfeifer P (2012) Activated carbon monoliths for methane storage. In: APS March Meeting Abstracts, vol 2012, pp W33-012
19. Soo Y, Chada N, Beckner M, Romanos J, Burress J, Pfeifer P (2013) Adsorbed methane film properties in nanoporous carbon monoliths. In: APS March Meeting Abstracts, vol 2013, pp M38-001
20. Bailey S, Olin T, Bricka M, Adrian D (1999) A review of potentially low-cost sorbents for heavy metals. Water Res 33:2469–2479
21. Babel S, Kurniawan T (2003) Low-cost adsorbents for heavy metals uptake from contaminated water: a review. J Hazard Mater 28:219–243
22. Huang MR, Huang SJ, Li XG (2011) Facile synthesis of polysulfoaminoanthraquinone nanosorbents for rapid removal and ultrasensitive fluorescent detection of heavy metal ions. J Phys Chem C 115(13):5301–5315
23. Shaban M, AbuKhadra MR, Nasief FM, Abd El-Salam HM (2017) Removal of ammonia from aqueous solutions, ground water, and wastewater using mechanically activated clinoptilolite and synthetic zeolite-a: kinetic and equilibrium studies. Water Air Soil Pollut 228(11):450
24. Abd El-Salam HM, Kamal EH, Ibrahim MS (2017) Synthesis and characterization of chitosan-grafted-poly (2-hydroxyaniline) microstructures for water decontamination. J Polymer Environ 25(4):973–982
25. Karthikeyan G, Anbalagan K, Andal NM (2004) Adsorption dynamics and equilibrium studies of Zn (II) onto chitosan. J Chem Sci 116(2):119–127
26. Boundy RH, Boyer RF (1952) Styrene: its copolymers and derivatives. Reinhold, New York, p 523
27. Ohtsuka Y, Kawaguchi H, Sugi Y (1981) Copolymerization of styrene with acrylamide in an emulsifier-free aqueous medium. J Appl Polymer Sci 26:1637–1647
28. Li LX, Song HH, Zhang QC, Yao JY, Chen XH (2009) Effect of compounding process on the structure and electrochemical properties of ordered mesoporous carbon/polyaniline composites as electrodes for supercapacitors. J Power Sources 187:268–274
29. Mu SL (2006) Catechol sensor using poly (aniline-co-o-aminophenol) as an electron transfer mediator. Biosens Bioelectron 21:1237–1243
30. Mu SL (2006) Novel properties of polyaniline nanofibers coated with polycatechol. Synth Met 156:202–208
31. Huang JX, Kaner RB (2006) The intrinsic nanofibrillar morphology of polyaniline. Chem Commun 4:367–376
32. Baker CO, Huang X, Nelson W, Kaner RB (2017) Polyaniline nanofibers: broadening applications for conducting polymers. Chem Soc Rev 46(5):1510–1525
33. Zare EN, Makvandi P, Ashtari B, Rossi F, Motahari A, Perale G (2019) Progress in conductive polyaniline-based nanocomposites for biomedical applications: a review. J Med Chem 63(1):1–22
34. Qu K, Bai Y, Gao X, Deng M (2020) Application of poly (aniline-co-o-methoxyaniline) as energy storage material. Synth Metals 262:116346
35. Gupta RK, Singh RA, Dubey SS (2004) Removal of mercury ions from aqueous solutions by composite of polyaniline with polystyrene. Purif Technol 38:225–232
36. Mansour MS, Ossman ME, Farag HA (2011) Removal of Cd (II) ion from waste water by adsorption onto polyaniline coated on sawdust. Desalination 272(1–3):301–305
37. Karthik R, Meenakshi S (2015) Removal of Pb (II) and Cd (II) ions from aqueous solution using polyaniline grafted chitosan. Chem Eng J 263:168–177
38. Eskandari E, Kosari M, Farahani MHDA, Khiavi ND, Saeedikhani M, Katal R, Zarinejad M (2020) A review on polyaniline-based materials applications in heavy metals removal and catalytic processes. Sep Purif Technol 231:115901
39. Abd El-Salam HM, Kamal EH, Ibrahim MS (2018) Cleaning of wastewater from total coliform using chitosan–grafted–poly (2-methylaniline). J Polymer Environ 26(8):3412–3421
40. Ibrahim MS, Abd El-Mageed HR, Abd El-Salam HM (2019) Density functional theory calculations on the grafting copolymerization of 2-substituted aniline onto chitosan. Polymer Bull 77:1–17
41. Abd El-Mageed HR, Abd El-Salam HM, Abdel-Latif MK, Mustafa FM (2018) Preparation and spectroscopic properties, density functional theory calculations and nonlinear optical properties of poly (acrylic acid-co-acrylamide)-graft-polyaniline. J Mol Struct 1173:268–279
42. Abd El-Mageed HR, Abd El-Salam HM, Eissa MF (2018) Spectroscopic study on poly (acrylicacid-co-acrylamide)-graft–polyaniline as a radiation dosimeter for alpha particles. Radiat Prot Dosim 178(4):374–381
43. Abd El-Salam HM, Mohamed RA, Shokry A (2019) Facile polyacrylamide graft based on poly (2-chloroaniline) silver nano-composites as antimicrobial. Int J Polym Mater Polym Biomater 68(5):278–286
44. Abd El-Salam HM, Mohamed RA, Shokry A (2018) Preparation and characterization of novel and selective polyacrylamide-graft-poly (2-methoxyaniline) adsorbent for lead removal. Polymer Bull 75(7):3189–3210
45. Oketola A, Torto N (2013) Synthesis and characterization of poly (styrene-co-acrylamide) polymers prior to electrospinning. Adv Nanopart 2:87–93
46. Khan H, Ahmed MJ, Bhanger MI (2005) A simple spectrophotometric determination of trace level mercury using 1,5-diphenylthiocarbazone solubilized in micelle. Anal Sci 21(5):507–512
47. Rojas C, Cea M, Iriarte A, Valdés G, Navia R, Cárdenas-R JP (2019) Thermal insulation materials based on agricultural residual wheat straw and corn husk biomass, for application in sustainable buildings. Sustain Mater Technol 20:e00102
48. Trchova M, Sedenkova I, Konyushenko EN, Stejskal J, Holler P, Ciric-Marjanovic G (2006) Evolution of polyaniline nanotubes: the oxidation of aniline in water. J Phys Chem B 110(19):9461–9468
49. Kang ET, Neoh KG, Tan KL (1998) Polyaniline: a polymer with many interesting intrinsic redox states. Prog Polymer Sci 23(2):277–324
50. Furukawa Y, Ueda F, Hyodo Y, Harada I, Nakajima T, Kawagoe T (1988) Vibrational spectra and structure of polyaniline. Macromolecules 21:1297
51. Sedenkova I, Trchova M, Blinova NV, Stejskal J (2006) In-situ polymerized polyaniline films. Preparation in solutions of hydrochloric, sulfuric, or phosphoric acid. Thin Solid Films 515(4):1640–1646
52. Socrates G (2001) Infrared and Raman characteristic group frequencies, pp 107–113, 122–123, 157–167, 176–177, 220–222. Wiley, New York
53. Bellamy L (1964) The infra-red spectra of complex molecules (No. 544.6 B45), pp 65–84, pp 249–261
54. Vien DL, Colthup NB, Fateley WG, Grasselli JG (1991) The handbook of infrared and Raman characteristic frequencies of organic molecules. Elsevier, Amsterdam, pp 277–299
55. Dan-asabe B, Yaro AS, Yawas DS, Aku SY, Samotu IA, Abubakar U, Obada DO (2016) Mechanical, spectroscopic and micro-structural

characterization of banana particulate reinforced PVC composite as piping material. Tribol Ind 38:255–267
56. Reddy KR, Lee KP, Gopalan AI (2007) Novel electrically conductive and ferromagnetic composites of poly (aniline-coaminonaphthalene sulfonic acid) with iron oxide nanoparticles:synthesis and characterization. J Appl Polymer Sci 106:1181–1191
57. Tang J, Jing X, Wang B, Wang F (1988) Infrared spectra of soluble polyaniline. Synth Met 24(3):231–238
58. Neto N, Ambrosino F, Califano S (1964) Vibrational assignment of phenazine-d8: crystal spectra of polarized light and force constants calculations. Spectrochim Acta 20(10):1503
59. Boyer ML, Quillard S, Louarn G, Froyer G, Lefrant S (2000) vibrational study of the $FeCl_3$-doped dimer of polyaniline; a good model compound of emeraldine salt. J Phys Chem B 104(38):8952–8961
60. Abd El-Salam HM, Abd El-Hafez GM, Askalany HG, Fekry AM (2020) A creation of poly (N-2-hydroxyethylaniline-co-2-chloroaniline) for corrosion control of mild steel in acidic medium. J Bio- Tribo-Corros 6(2):1–14
61. Alshameri A, Ibrahim A, Assabri AM, Lei XR, Wang HQ, Yan CJ (2014) The investigation into the ammonium removal. performance of Yemeni natural zeolite: modification, ion exchange mechanism, and thermodynamics. Powder Technol 258:20–31
62. Hui KS, Chao CYH, Kot SC (2005) Removal of mixed heavy metal ions in wastewater by zeolite 4A and residual products from recycled coal fly ash. J Hazard Mater 127:89–101
63. Namasivayam C, Yamuna RT (1995) Adsorption of direct red 12 B by biogas residual slurry: equilibrium and rate processes. Environ Pollut 89:1–7
64. Freundlich I, Helle WJ (1939) Flubber die adsorbtion in lusungen. J Am Chem Soc 61:2–28
65. Temkin MJ, Pyzhev V (1940) Kinetics of ammonia synthesis on promoted iron catalysts. Acta Physiochim URSS 12:217–222
66. Lagergren SY (1898) Zur Theorie der sogenannten adsorption geloster stoffe. Kungl Svenska Vetenskapsakad Handl 25:1–39
67. Ho YS, McKay G (1999) Pseudo-second-order model for sorption processes. Process Biochem 34:451–465

Publisher's Note